Concatenation of Hamming Codes and Accumulator Codes with High-Order Modulations for High-Speed Decoding

D. Divsalar[1] and S. Dolinar[1]

We propose a concatenated code structure combined with high-order modulations suitable for implementation with iterative decoders operating at gigabit-per-second (Gbps) data rates. The examples considered in this article are serial/parallel concatenations of Hamming and accumulator codes. Performance results are given for binary phase-shift keyed (BPSK) modulation, quadrature phase-shift keyed (QPSK) modulation, 8 phase-shift keyed (8PSK) modulation, and 16 quadrature amplitude modulation (16QAM) over additive white Gaussian noise (AWGN) and Rayleigh fading channels.

I. Introduction

In this article, we design coding schemes based on serial concatenations [7,10] of a high-rate Hamming outer code and a simple 2-state, rate-1 accumulator inner code. The interleaver between the outer and inner codes has a block structure that allows easy parallelization of the decoding algorithm for applications requiring high-speed decoding. The serially concatenated codes are combined with binary phase-shift keyed (BPSK) modulation, quadrature phase-shift keyed (QPSK) modulation, 8 phase-shift keyed (8PSK) modulation, or 16 quadrature amplitude modulation (16QAM) to give high overall bandwidth efficiencies.

The general structure of a serial concatenation with a "parallel interleaver" is shown in Fig. 1. In this construction of an $(n^O n^I, k^O k^I)$ code, we concatenate k^I outer codes $\{\mathcal{C}_i^O, i = 1, \cdots, k^I\}$ of length and dimension (n^O, k^O) with n^O inner codes $\{\mathcal{C}_j^I, j = 1, \cdots, n^O\}$ of length and dimension (n^I, k^I), via an interleaver π of total size $k^I n^O$. Instead of allowing a completely general interleaver of size $k^I n^O$, we require that π be decomposable into a set of permutations $\{\pi_i^O, i = 1, \cdots, k^I\}$, each of size n^O, applied to the outputs of each of the k^I outer codes separately, followed by a $k^I \times n^O$ rectangular interleaver, followed by a set of permutations $\{\pi_j^I, j = 1, \cdots, n^O\}$, each of size k^I, applied to the inputs of each of the n^O inner codes separately. In the interests of allowing more irregularity, this structure can be generalized to allow the outer codes $\{\mathcal{C}_i^O, i = 1, \cdots, k^I\}$ to have different dimensions $\{k_i^O, i = 1, \cdots, k^I\}$ and the inner codes $\{\mathcal{C}_j^I, j = 1, \cdots, n^O\}$ to have different lengths $\{n_j^I, j = 1, \cdots, n^O\}$; however, in this article, our attention is restricted to component codes with non-varying dimensions and lengths.

---

[1] Communications Systems and Research Section.

The research described in this publication was carried out by the Jet Propulsion Laboratory, California Institute of Technology, under a contract with the National Aeronautics and Space Administration.

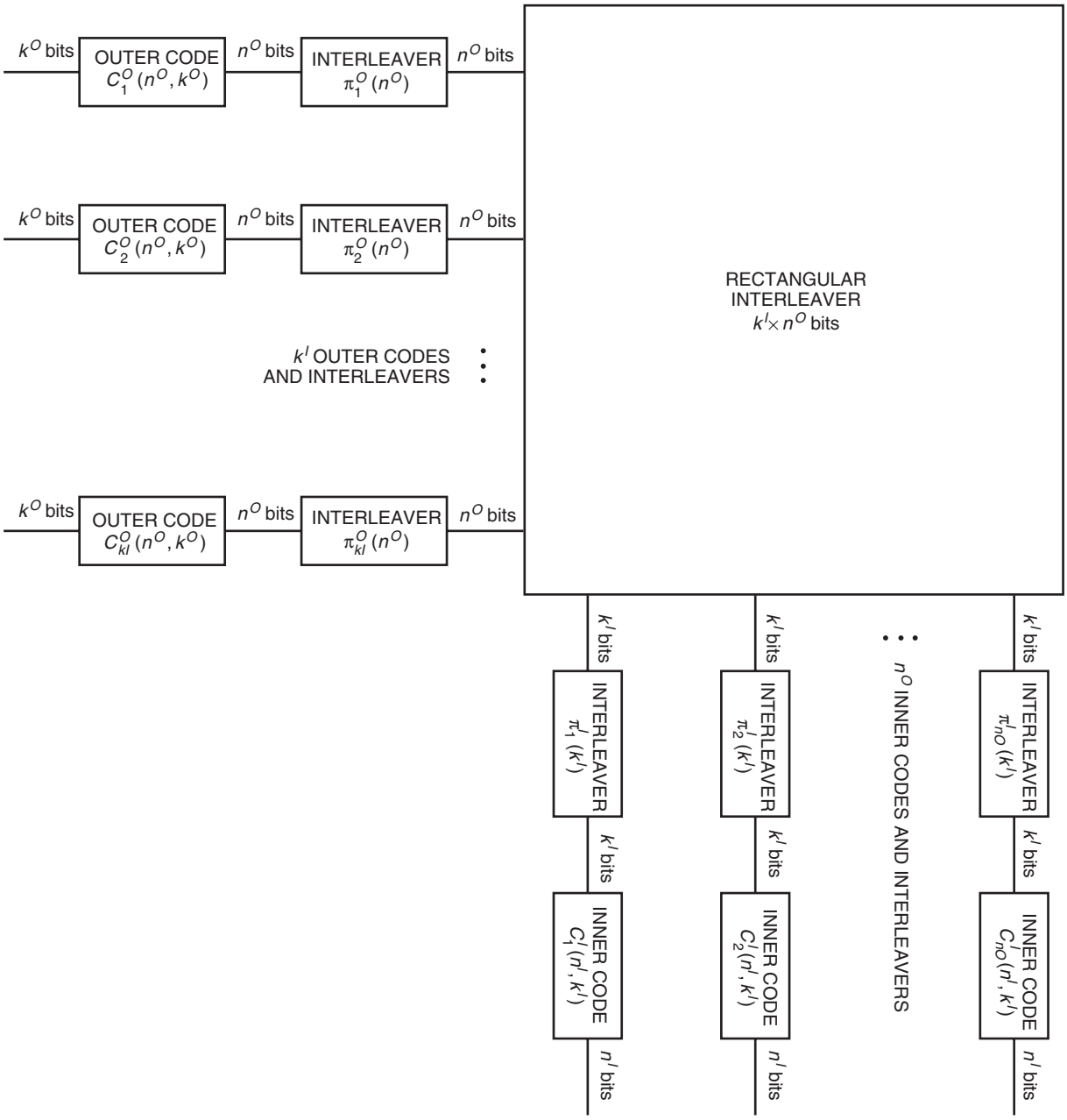

Fig. 1. Serial concatenation with parallel interleaver structure.

This structure gives a natural generalization of parallel concatenated codes [11], rather than just an interesting subclass of serially concatenated codes. To see this, simply let all of the k^I outer codes be $(q, 1)$ repetition codes. In this case, the interleavers at the outputs of the outer codes have no effect and can be omitted. The rectangular interleaver simply ensures that each of the $n^O = q$ inner codes receives a copy of the full package of k^I distinct input bits. Then the random interleavers at the inputs of the inner codes feed different permutations of these k^I bits to each inner code. The net effect is the same as the usual definition of a parallel concatenated (turbo) code.

When the outer codes are not repetition codes, the interleavers attached to the outer codes can provide some interleaving gain, although this gain will be fairly small if the outer codes are small block codes.

For example, an (8,4) extended Hamming outer code has 14 codewords of weight 4. After a random permutation, each of these 14 codewords could be scattered into any of $\binom{8}{4} = 70$ weight-4 sequences of length 8. This effectively thins the weight-4 part of the Hamming code's weight spectrum by a factor of $70/14 = 5$.

We were interested in the case where the outer component codes $\{\mathcal{C}_i^O, i = 1, \cdots, k^I\}$ are small Hamming codes or extended Hamming codes, and the inner codes are 2-state, rate-1 accumulator codes [1]. Our aim was to produce codes with good power and bandwidth efficiencies, over a range of bandwidth utilizations, that can be decoded with parallel architecture at very high speeds, on the order of 1 gigabit per second (Gbps). We wanted outer codes with high code rates for teaming with high-order modulations and with minimum distance 3 or 4 to achieve high interleaving gain. These considerations led to our choice of Hamming or extended Hamming codes as the outer codes that could achieve minimum distance 3 or 4 with the highest code rates for given code dimensions. For the inner codes, we selected 2-state, rate-1 accumulator codes $1/(1+D)$ for their extreme simplicity of decoding. Since the accumulator codes have the same complexity per bit independent of their length, whereas the decoding complexity of the Hamming codes increases with their lengths, the overall design is asymmetric in the number and sizes of the outer and inner codes, specifically, $n^O \ll k^I$. A goal is to select these sizes such that k^I parallel copies of the outer decoder can run at approximately the same speed as n^O parallel copies of the inner decoder.

II. Coded Modulations Using the (15,11) Hamming and Accumulator Codes

In this article, we concentrate on one example of the general structure in Fig. 1 in which the outer codes are (15,11) Hamming codes. We team this rate-11/15 code with QPSK modulation, 8PSK modulation, or 16QAM, producing (ideal) bandwidth efficiencies of 1.47 bps/Hz, 2.20 bps/Hz, and 2.93 bps/Hz, respectively.

Figure 2 shows the encoder for a (15,11) Hamming outer code concatenated with a 2-state, rate-1 accumulator inner code. For this code, $k^O = 11$, $n^O = 15$, and we selected $k^I = n^I = 372$ to yield an overall code of length 5580 and dimension 4092. In our implementation, we used $k^I = 372$ random interleavers $\{\pi_i^O, i = 1, \cdots, n^O\}$ at the output of the Hamming outer codes and $n^O = 372$ S-random [2] interleavers $\{\pi_j^I, j = 1, \cdots, k^I\}$ to permute the inputs to the accumulator inner codes. In the figure, we indicate that a desired input data rate of 1.116 Gbps can be obtained by running the 372 Hamming encoders at 3 Mbps each and the 15 accumulator encoders at 101 Mbps each.

The outputs of the 15 accumulator codes are mapped to a high-order modulation. With 8PSK, the first output bits of the first three accumulators are mapped to a 3-bit 8PSK symbol using a Gray code mapping. Then the first output bits of the next three accumulators are mapped to the second 3-bit 8PSK symbol, and so on, until the first five 8PSK symbols are produced. Then the next five 8PSK symbols are created using the second bits from three accumulators at a time, and so forth. With QPSK or 16QAM, we take output bits two or four at a time from two or four separate accumulators to form each QPSK or 16QAM symbol, stepping through the 15 accumulator codes in a cyclic order until all 5580 output bits are mapped. This type of mapping eliminates the need for a channel interleaver within the length of a code block.

Figure 3 shows the decoder for the code in Fig. 2. In this figure, the demapper provides the reliability of those bits assigned to the modulation symbols, given in-phase and quadrature received observations. The soft-in, soft-out (SISO) modules [8,9] for the accumulator also can interact with the demapper for further performance enhancement if desired.

An (n, k) Hamming code has a cyclic representation and can be equivalently generated as a recursive terminated convolutional code with primitive feedback polynomial. If the feedforward polynomial is chosen to be the same as the feedback polynomial, this produces a systematic version of the Hamming

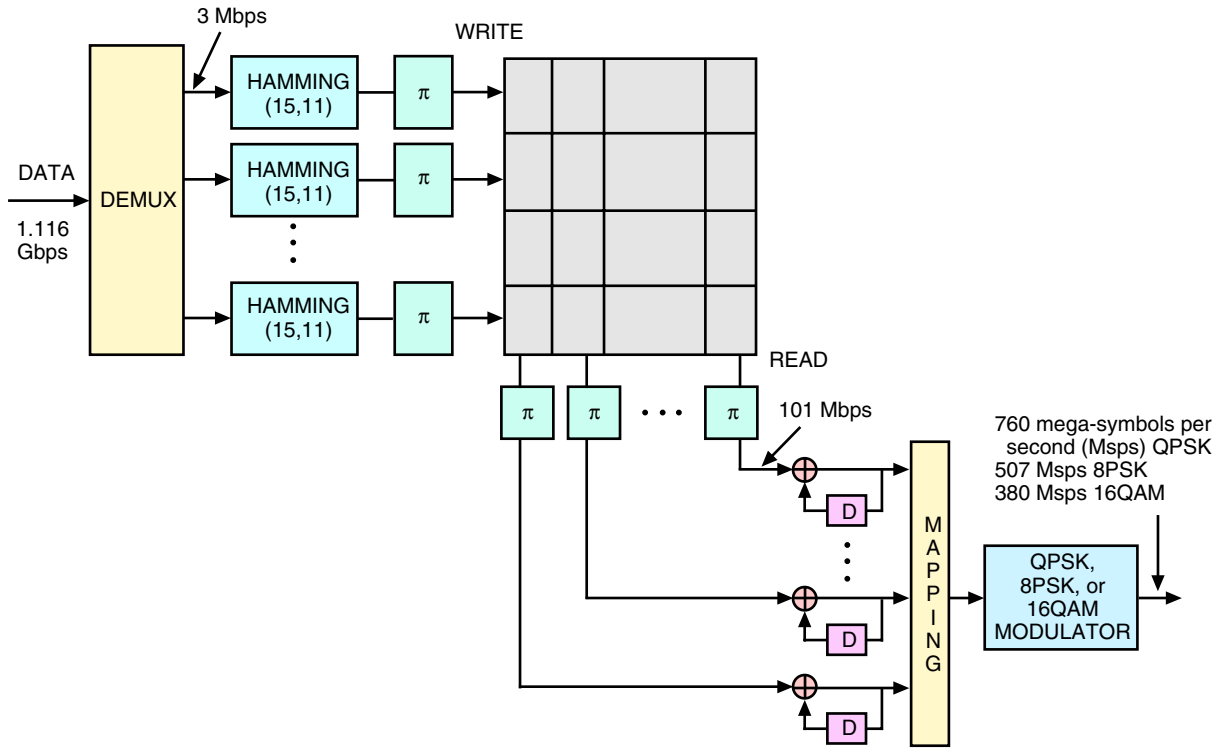

Fig. 2. Encoder for the Hamming and accumulator code.

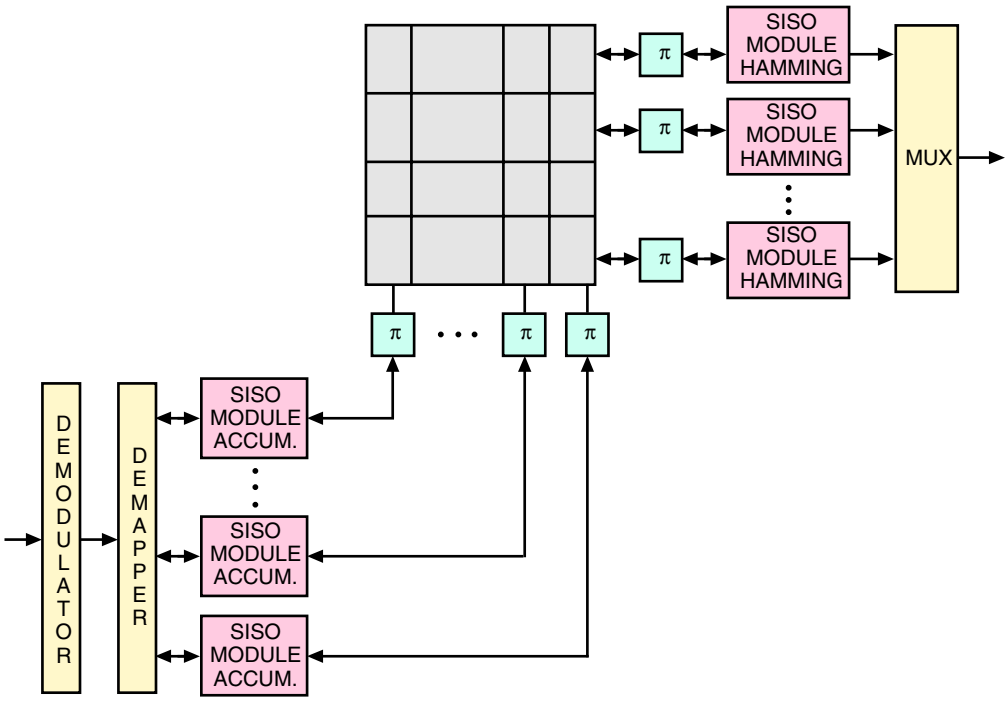

Fig. 3. Decoder for the Hamming and accumulator code.

code. This convolutional encoding of the (15,11) Hamming code is shown in Fig. 4. The first k bits enter the systematic convolutional encoder and emerge as the first k encoded symbols. After k bits, the switch in Fig. 4 is toggled, and the encoder continues running long enough to produce $n-k$ additional encoded symbols, which are the parity symbols for the (n,k) Hamming code. We note that an extended Hamming code, shortened by one bit, also can be implemented by a recursive convolutional code, where the primitive feedback and feedforward polynomials are multiplied by $1+D$.

The convolutional encoding of an (n,k) Hamming code gives a time-invariant trellis representation with 2^{n-k} states. Alternatively, a time-varying minimal trellis representation can be used for decoding to gain speed if necessary over that provided by the time-invariant trellis representation. Figure 5 shows a minimal trellis representation for the (15,11) Hamming code. The time-invariant trellis corresponding to the convolutional encoder of Fig. 4 has 32 edges per decoded bit, whereas the time-varying trellis of Fig. 5 has only 17.8 trellis edges (on the average) per decoded bit, a reduction of nearly a factor of 2.

The inner accumulator code can be decoded using the Bahl–Cocke–Jelinek–Raviv (BCJR) algorithm [3,8,9] on a time-invariant trellis with only two states. Alternatively, the accumulator code also can be decoded using belief propagation on a loop-free Tanner graph [4] representing the same code, as shown in Fig. 6.

If higher speeds and many iterations are necessary, the inner or outer decoders can pipeline their iterations as needed.

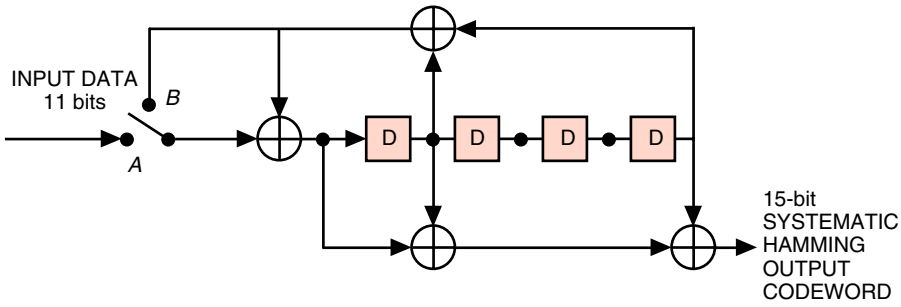

Fig. 4. A recursive convolutional code with primitive feedback polynomial that generates a time-invariant trellis representation that can be used for decoding the (15,11) Hamming code.

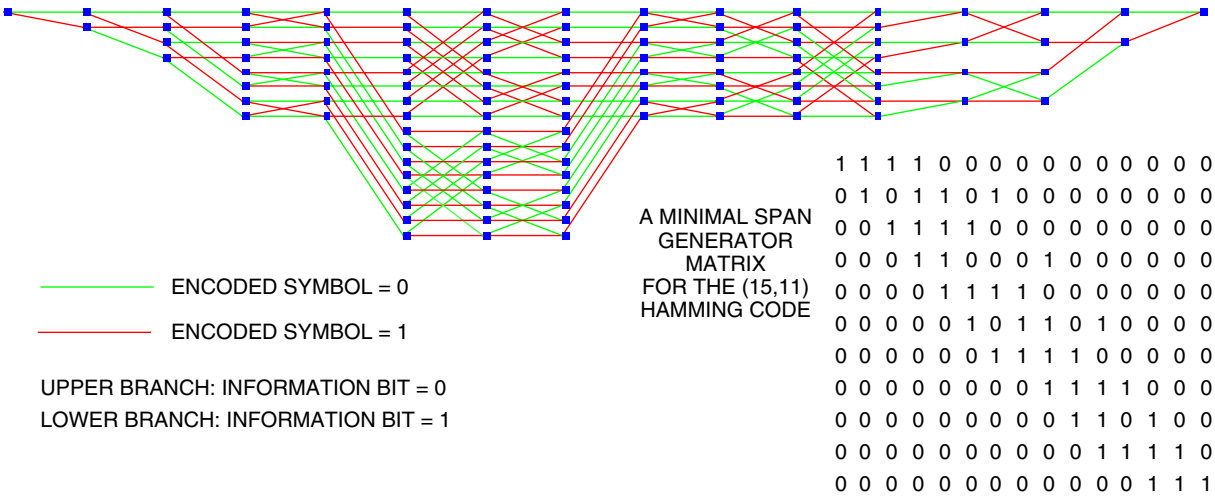

Fig. 5. A time-varying minimal trellis representation that can be used for decoding the (15,11) Hamming code.

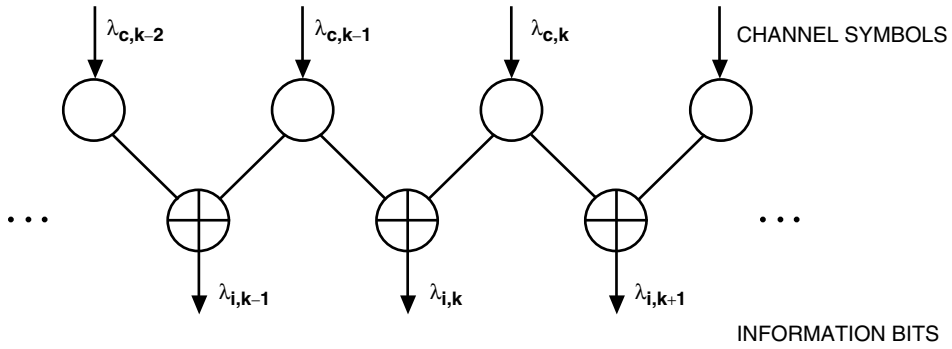

Fig. 6. A Tanner graph representation of the accumulator code that can be used for high-speed parallelizable decoding.

III. Performance on an Additive White Gaussian Noise Channel

First we applied Gaussian density evolution [5,6] (see also [12]) to analyze the performance of concatenated Hamming and accumulator codes under iterative decoding on an additive white Gaussian noise (AWGN) channel. The results are shown in Fig. 7, which plots the output signal-to-noise ratio $\mathrm{SNR}_{\mathrm{out}}$ versus the input signal-to-noise ratio $\mathrm{SNR}_{\mathrm{in}}$ of the extrinsic log-likelihood messages computed by the outer and inner component decoders. The iterative decoding threshold for this code on the binary-input AWGN channel is $E_b/N_0 = 2.1$ dB, which is only 0.6 dB worse than the capacity threshold of 1.505 dB for any code of rate 11/15.

Next we simulated the performance of the (5580,4092) Hamming and accumulator code when combined with various modulations. Figures 8 through 10 show the bit-error rate (BER) and codeword-error rate (WER) performance of this code with QPSK, 8PSK, and 16QAM, respectively, on the AWGN channel. The capacity thresholds for QPSK, 8PSK, and 16QAM are 1.505 dB, 3.47 dB, and 4.36 dB, at throughputs of 1.47 bps/Hz, 2.20 bps/Hz, and 2.93 bps/Hz, respectively.

IV. Performance on a Rayleigh Fading Channel

We applied Gaussian density evolution [5,6] to analyze the performance of concatenated Hamming and accumulator codes under iterative decoding on an independent Rayleigh fading channel with perfect channel state information. The results are shown in Fig. 11. The iterative decoding threshold for this code and channel is $E_b/N_0 = 5.5$ dB.

We simulated the performance of the (5580,4092) Hamming and accumulator code when combined with QPSK modulation, 8PSK modulation, and 16QAM on a correlated Rayleigh fading channel, where the ratio of the maximum Doppler rate f_d to the modulation transmission rate R_s is set as a parameter. The fading process was generated by passing a complex white Gaussian process through a filter with transform function $H(f) = \sqrt{S(f)}$, where $S(f)$ is the power spectral density of the fading process and is modeled for an omnidirectional antenna as $S(f) = C/\sqrt{1-(f/f_d)^2}$, where C is a constant; see Fig. 12.

Figures 13 through 15 show the BER and WER with QPSK, 8PSK, and 16QAM, respectively, and no channel interleaving, for $f_d/R_s = 0.05$. For slower fading, with f_d/R_s significantly less than 0.05, channel interleaving over multiple codewords is required to obtain good performance. The capacity thresholds for QPSK, 8PSK, and 16QAM over independent Rayleigh fading with perfect channel state information are 4.66 dB, 6.49 dB, and 7.25 dB, at throughputs of 1.47 bps/Hz, 2.20 bps/Hz, and 2.93 bps/Hz, respectively.

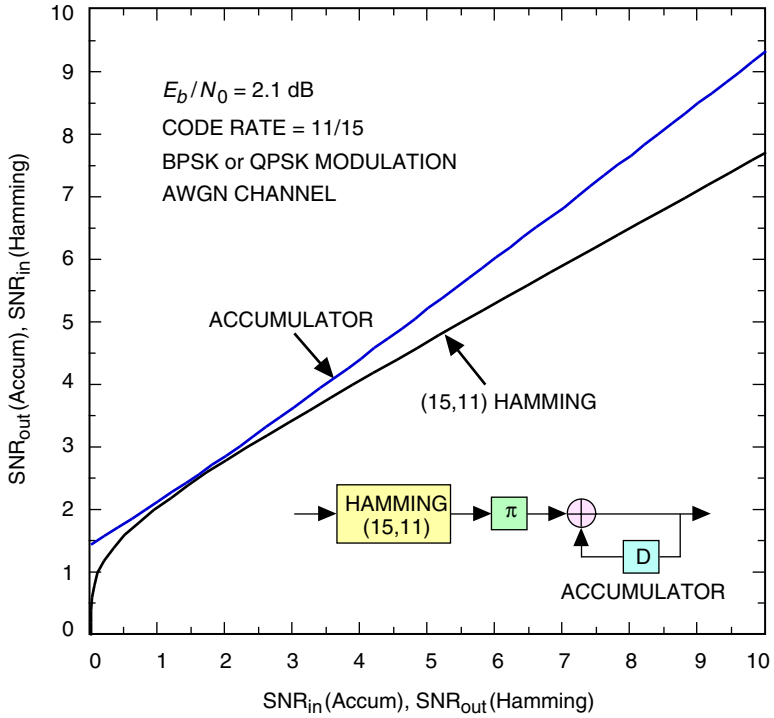

Fig. 7. Gaussian density evolution for the Hamming and accumulator code on the AWGN channel.

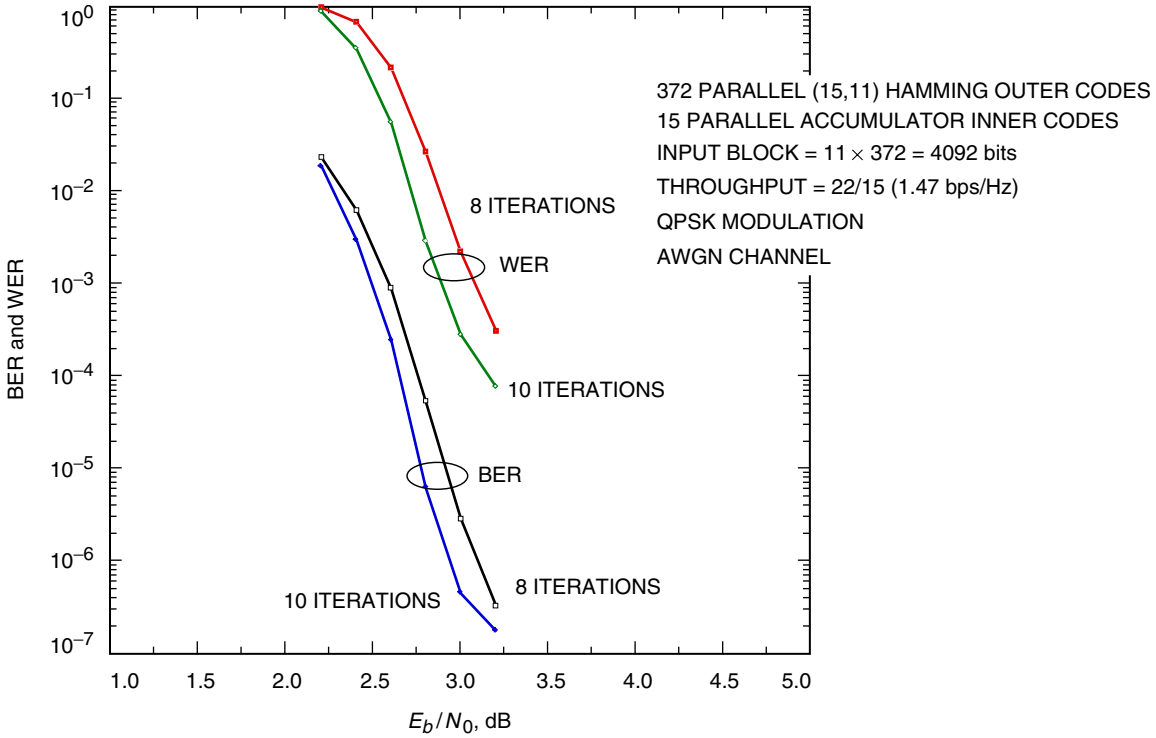

Fig. 8. Performance of the (15,11) Hamming code concatenated via a parallelized interleaver with the 2-state accumulator code, when combined with QPSK modulation on an AWGN channel.

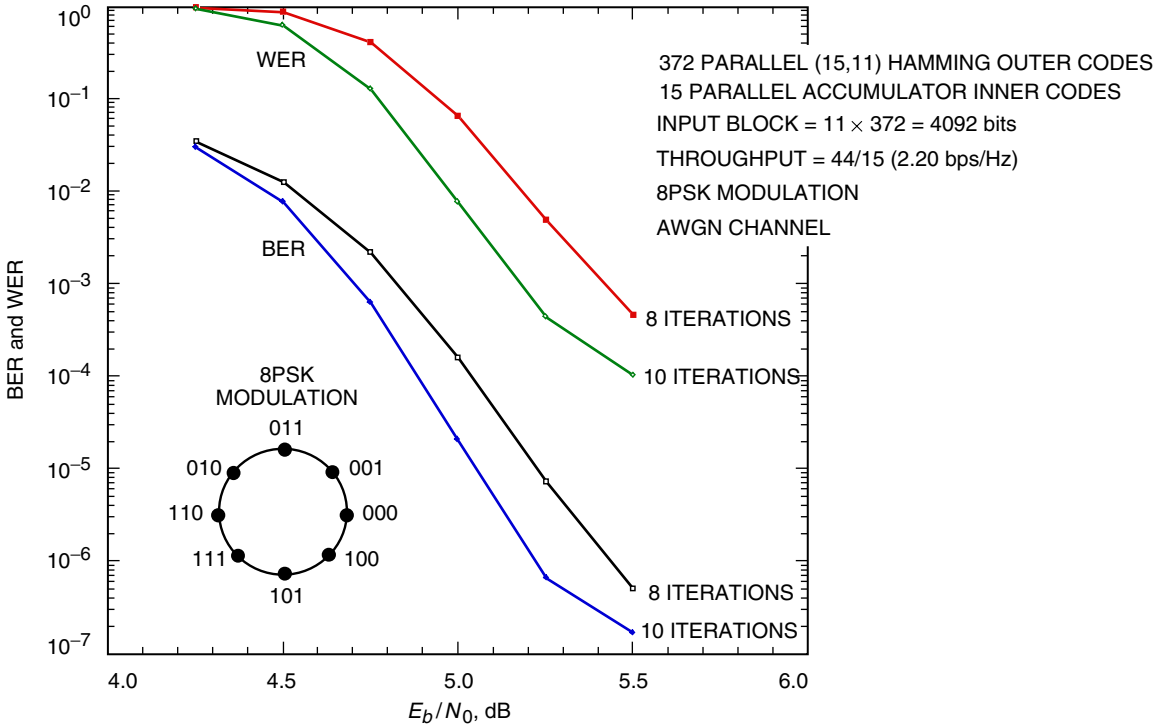

Fig. 9. Performance of the (15,11) Hamming code concatenated via a parallelized interleaver with the 2-state accumulator code, when combined with 8PSK modulation on an AWGN channel.

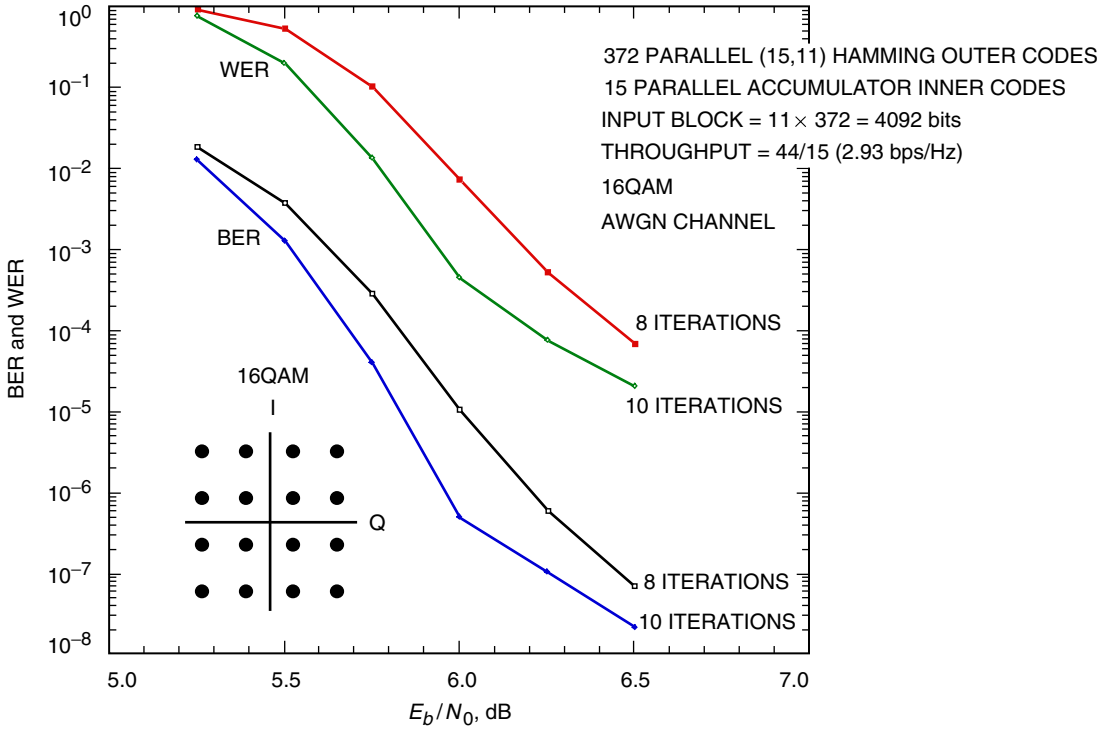

Fig. 10. Performance of the (15,11) Hamming code concatenated via a parallelized interleaver with the 2-state accumulator code, when combined with 16QAM on an AWGN channel.

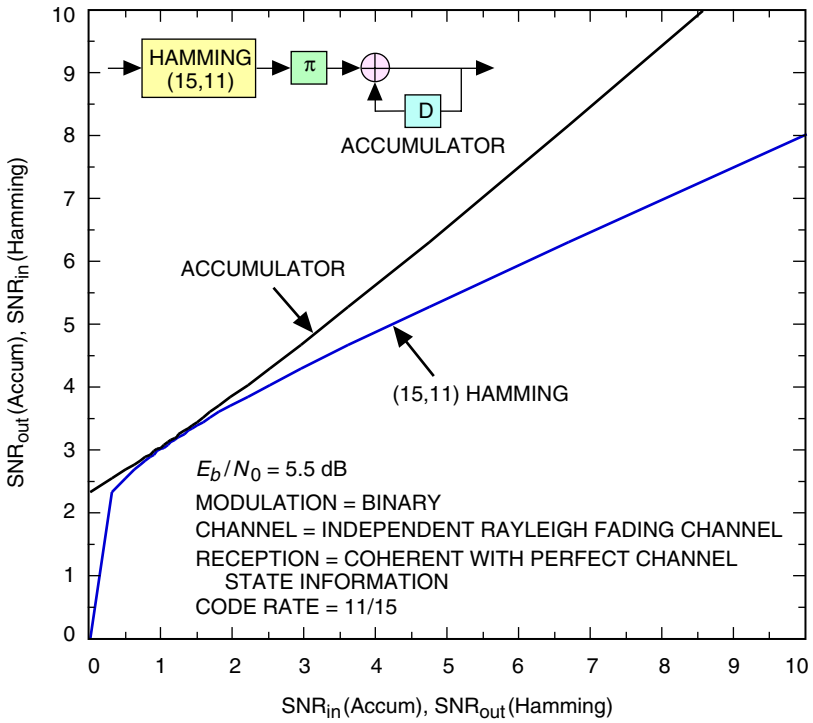

Fig. 11. Gaussian density evolution for the Hamming and accumulator code on an independent Rayleigh fading channel.

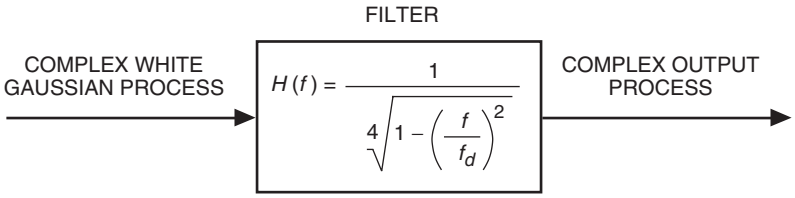

Fig. 12. Fading channel simulator to model a correlated Rayleigh fading channel.

V. Other Performance Examples Using Different Hamming Codes

Figure 16 shows performance with BPSK modulation over an AWGN channel for rate-1/2 codes with input block sizes $k = 1024, 4096, 16384$, formed from concatenating $k^I = 128, 512, 2048$ (8,4) Hamming outer codes with $n^O = 8$ accumulator codes. In this case, the minimum distance of the outer codes is 4, thus yielding higher interleaving gain. As seen in Fig. 16, very low word-error rates are achieved for the large block size, $k = 16384$, at E_b/N_0 of about 1.2 dB, which is about 1 dB above the capacity threshold for this code. The Shannon capacity limit of 0.187 dB also is shown in the figure.

Figure 17 shows performance with BPSK modulation over an AWGN channel for a very high-rate ($57/63 = 0.905$) code with input block size $k = 1824$, formed from concatenating $k^I = 32$ (63,57) Hamming outer codes with $n^O = 63$ accumulator codes. The Shannon capacity threshold for rate 57/63 is 3.27 dB.

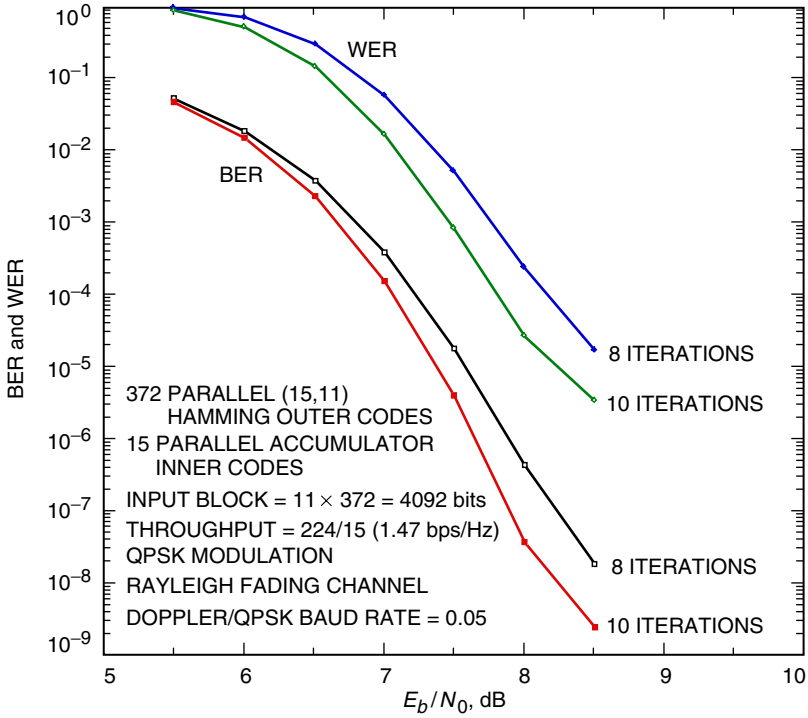

Fig. 13. Performance of the (15,11) Hamming code concatenated via a parallelized interleaver with the 2-state accumulator code, when combined with QPSK modulation on a correlated Rayleigh fading channel.

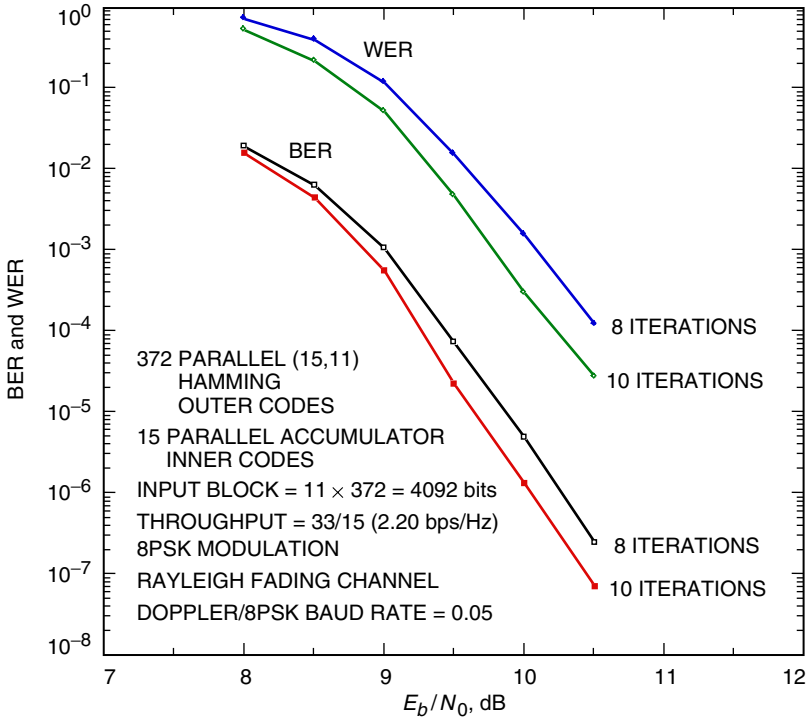

Fig. 14. Performance of the (15,11) Hamming code concatenated via a parallelized interleaver with the 2-state accumulator code, when combined with 8PSK modulation on a correlated Rayleigh fading channel.

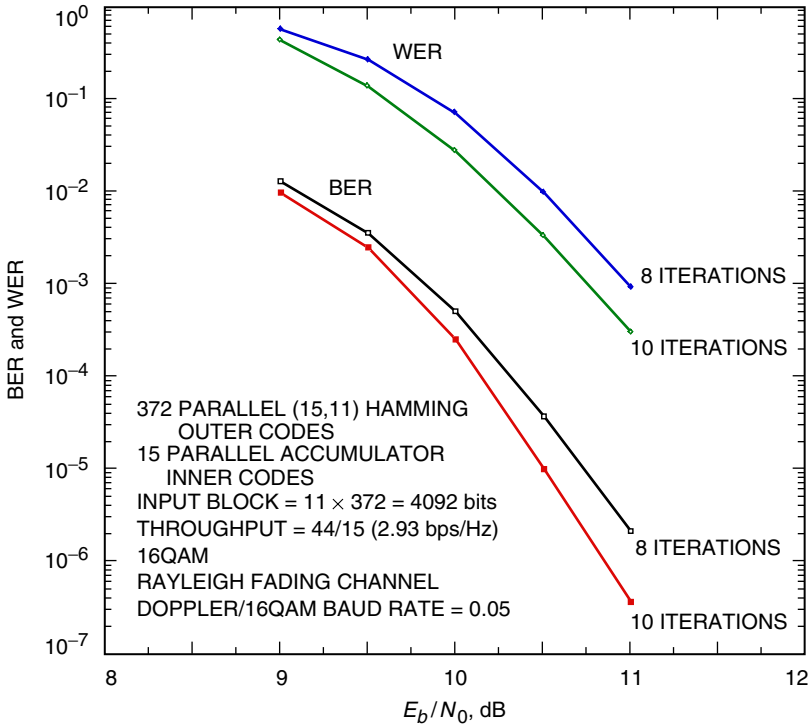

Fig. 15. Performance of the (15,11) Hamming code concatenated via a parallelized interleaver with the 2-state accumulator code, when combined with 16QAM on a correlated Rayleigh fading channel.

VI. Conclusion

The concatenated codes described in this article achieve medium to high code rates using very simple component codes and can be combined with high-order modulations to obtain good power and bandwidth efficiency at very high decoding rates.

References

[1] D. Divsalar, H. Jin, and R. J. McEliece, "Coding Theorems for 'Turbo-Like' Codes," 1998 Allerton Conference, September 23–25, 1998.

[2] S. Dolinar and D. Divsalar, "Weight Distributions for Turbo Codes Using Random and Nonrandom Permutations," *The Telecommunications and Data Acquisition Progress Report 42-122, April–June 1995*, Jet Propulsion Laboratory, Pasadena, California, pp. 56–65, August 15, 1995.
http://tmo.jpl.nasa.gov/tmo/progress_report/42-122/122B.pdf

[3] L. R. Bahl, J. Cocke, F. Jelinek, and J. Raviv, "Optimal Decoding of Linear Codes for Minimizing Symbol Error Rate," *IEEE Trans. Inform. Theory*, vol. IT-20, pp. 284–287, 1974.

[4] R. M. Tanner, "A Recursive Approach to Low Complexity Codes," *IEEE Transactions on Information Theory*, vol. 27, issue 5, pp. 533–547, September 1981.

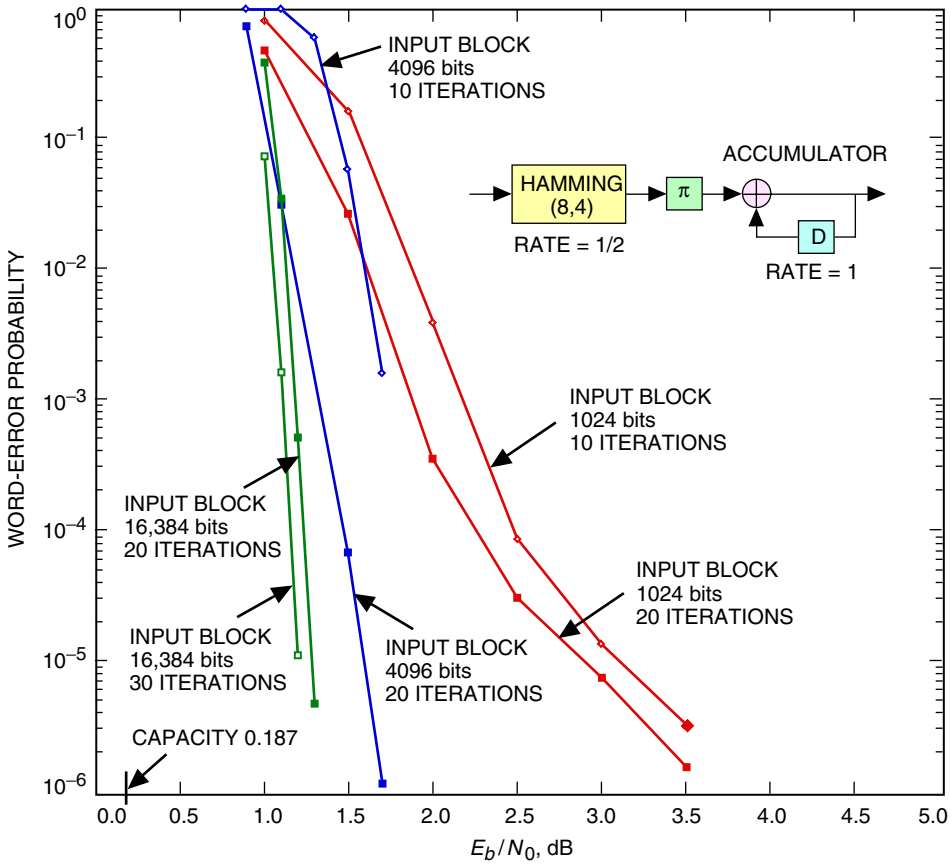

Fig. 16. Performance with BPSK modulation for a rate-1/2 code formed from concatenating an (8,4) Hamming outer code with the 2-state accumulator code.

[5] H. El Gamal and A. R. Hammons, Jr., "Analyzing the Turbo Decoder Using the Gaussian Approximation," *IEEE Transactions on Information Theory*, vol. 47, issue 2, pp. 671–686, February 2001.

[6] D. Divsalar, S. Dolinar, and F. Pollara, "Iterative Turbo Decoder Analysis Based on Density Evolution," *IEEE Journal on Selected Areas in Communications*, vol. 19, no. 5, pp. 891–907, May 2001.

[7] S. Benedetto, D. Divsalar, G. Montorsi, and F. Pollara, "Serial Concatenation of Interleaved Codes: Performance Analysis, Design, and Iterative Decoding," *IEEE Transactions on Information Theory*, vol. 44, pp. 909–926, May 1998.

[8] S. Benedetto, D. Divsalar, G. Montorsi, and F. Pollara, "A Soft-Input Soft-Output Maximum A Posteriori (MAP) Module to Decode Parallel and Serial Concatenated Codes," *The Telecommunications and Data Acquisition Progress Report 42-127, July–September 1996*, Jet Propulsion Laboratory, Pasadena, California, pp. 1–20, November 15, 1996.
http://tmo.jpl.nasa.gov/tmo/progress_report/42-127/127H.pdf

[9] S. Benedetto, D. Divsalar, G. Montorsi, and F. Pollara, "A Soft-Input Soft-Output APP Module for Iterative Decoding of Concatenated Codes," *IEEE Communications Letters*, vol. 1, issue 1, pp. 22–24, January 1997.

[10] D. Divsalar, S. Dolinar, and F. Pollara, "Serial Concatenated Trellis Coded Modulation with Rate-1 Inner Code," Global Telecommunications Conference, 2000, *GLOBECOM '00, IEEE*, vol. 2, no. 27, November 27–December 1, 2000, pp. 777–782.

[11] C. Berrou and A. Glavieux, "Near Optimum Error Correcting Coding and Decoding: Turbo-Codes," *IEEE Transactions on Communications*, vol. 44, issue 10, pp. 1261–1271, October 1996.

[12] S. ten Brink, "Convergence Behavior of Iteratively Decoded Parallel Concatenated Codes," *IEEE Transactions on Communications*, vol. 49, issue 10, pp. 1727–1737, October 2001.

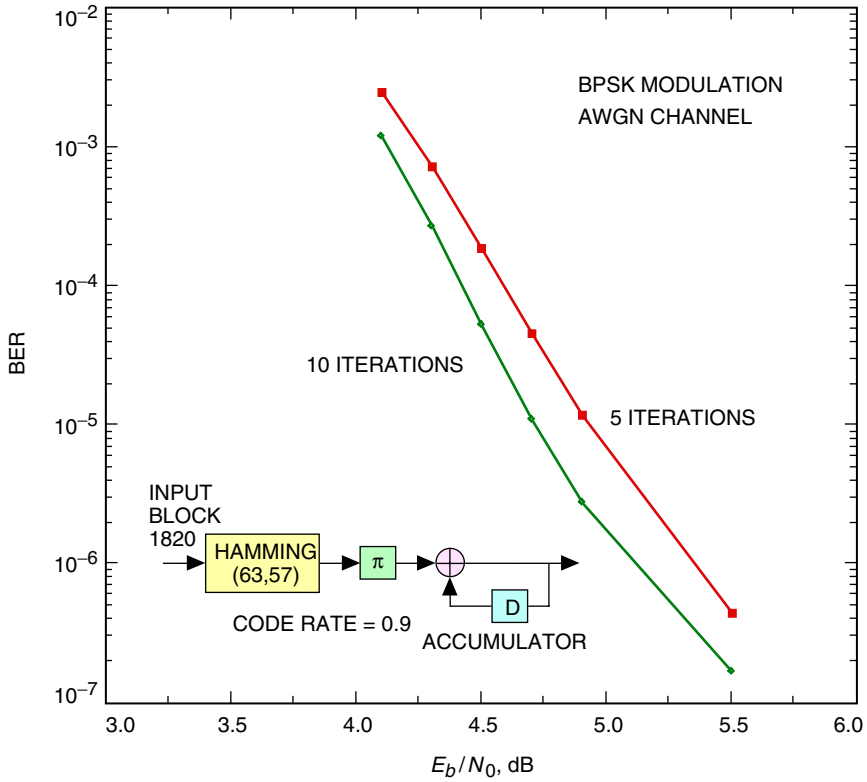

Fig. 17. Performance with BPSK modulation for a very high rate code formed from concatenating a (63,57) Hamming outer code with a 2-state, rate-1 accumulator inner code.